

## **General Disclaimer**

### **One or more of the Following Statements may affect this Document**

- This document has been reproduced from the best copy furnished by the organizational source. It is being released in the interest of making available as much information as possible.
- This document may contain data, which exceeds the sheet parameters. It was furnished in this condition by the organizational source and is the best copy available.
- This document may contain tone-on-tone or color graphs, charts and/or pictures, which have been reproduced in black and white.
- This document is paginated as submitted by the original source.
- Portions of this document are not fully legible due to the historical nature of some of the material. However, it is the best reproduction available from the original submission.



## Technical Memorandum 79609

### Diffuse Fluxes of Cosmic High Energy Neutrinos

(NASA-TM-79609) DIFFUSE FLUXES OF COSMIC  
HIGH ENERGY NEUTRINOS (NASA) 30 P HC A03/HF  
A01 CSCI 03E

N78-31040

Unclas  
G3/93 29420

F. W. Stecker



JULY 1978

National Aeronautics and  
Space Administration

**Goddard Space Flight Center**  
Greenbelt, Maryland 20771

**Diffuse Fluxes of Cosmic High Energy Neutrinos**

**F. W. Stecker  
Laboratory for High Energy Astrophysics  
NASA/Goddard Space Flight Center**

Received \_\_\_\_\_

## 1. Introduction

There have been a number of recent papers estimating high-energy neutrino fluxes and spectra from various astrophysical processes (Berezinsky and Zatsepin 1970, Stecker 1973a, Berezinsky and Zatsepin 1977 and references therein, Silberberg and Shapiro 1977, Margolis, Schramm and Silberberg 1978, Eichler 1978.) In this work, I reexamine the problem by 1) presenting the results of a detailed calculation of galactic  $\nu$ -production in cosmic-ray interactions with interstellar gas and extragalactic  $\nu$ -production by interactions of ultrahigh energy cosmic rays with the 3K universal background radiation, 2) using these results together with present  $\gamma$ -ray observations to predict neutrino fluxes and event rates, and 3) reexamining some of the assumptions and results of previous work, pointing out significant differences.

## 2. Production Rates

The first basic production process for high energy cosmic neutrinos is the decay of charged pions produced in cosmic ray interactions with interstellar gas, primarily pp interactions. This process will henceforth be referred to as "pp", although the effects of  $\alpha p$  pHe and  $\alpha$ He interactions are included in the calculation. The second process involves the photo-production of  $\pi$ -mesons by interaction of ultrahigh energy cosmic rays with the 3K universal microwave background radiation (henceforth referred to as  $\gamma p$ ) and subsequent meson decay. Both of these types of interactions involve the accompanying production of  $\pi^0$  mesons and their decay into cosmic  $\gamma$ -rays. Thus, the production rates of cosmic  $\gamma$ -rays and neutrinos are generically linked.

A detailed discussion of the kinematics of the production and decay of secondary particles produced in "pp" interactions may be found in Stecker

## 1. Introduction

There have been a number of recent papers estimating high-energy neutrino fluxes and spectra from various astrophysical processes (Berezinsky and Zatsepin 1970, Stecker 1973a, Berezinsky and Zatsepin 1977 and references therein, Silberberg and Shapiro 1977, Margolis, Schramm and Silberberg 1978, Eichler 1978.) In this work, I reexamine the problem by 1) presenting the results of a detailed calculation of galactic  $\nu$ -production in cosmic-ray interactions with interstellar gas and extragalactic  $\nu$ -production by interactions of ultrahigh energy cosmic rays with the 3K universal background radiation, 2) using these results together with present  $\gamma$ -ray observations to predict neutrino fluxes and event rates, and 3) reexamining some of the assumptions and results of previous work, pointing out significant differences.

## 2. Production Rates

The first basic production process for high energy cosmic neutrinos is the decay of charged pions produced in cosmic ray interactions with interstellar gas, primarily pp interactions. This process will henceforth be referred to as "pp", although the effects of  $\alpha p$  pHe and  $\alpha$ He interactions are included in the calculation. The second process involves the photo-production of  $\pi$ -mesons by interaction of ultrahigh energy cosmic rays with the 3K universal microwave background radiation (henceforth referred to as  $\gamma p$ ) and subsequent meson decay. Both of these types of interactions involve the accompanying production of  $\pi^0$  mesons and their decay into cosmic  $\gamma$ -rays. Thus, the production rates of cosmic  $\gamma$ -rays and neutrinos are generically linked.

A detailed discussion of the kinematics of the production and decay of secondary particles produced in "pp" interactions may be found in Stecker

(1971). Details of the  $\gamma p$  process have also been previously given (Stecker 1968). The  $\gamma$ -ray production spectrum in  $\gamma p$  interactions has been calculated by Wdowczyk et al. (1972), Stecker and Bredekamp (1972), and Stecker (1973a).

In the present paper, the "pp" neutrino production spectrum was calculated for pp interactions up to 30 GeV by methods previously employed (Stecker 1971, 1973b). At higher energies, scaling was assumed to hold. At these energies, the parameters of Ganguli and Sreekantan (1976) were adopted for the rapidity distribution of charged pions. These authors have calculated  $\gamma$ -ray spectra which are in good agreement with those of Stecker (1970) for  $\gamma$ -ray energies  $\leq 10$  GeV, however, at higher energies, the assumption of scaling gives larger fluxes and a flatter spectrum than those calculated by Stecker (1971) using an "isobar + fireball" model in "pre-scaling days". It should be noted that the isobar + fireball (I-F) model is equivalent to a "leading-pion" model at high energies, since the isobar carries off  $\sim 50\%$  of the energy and decays into a "leading pion". Both scaling and the I-F models produce a secondary spectrum which has the same spectral index as the primary spectrum in the high-energy limit. (See Appendix I).

The results of the "pp" production spectrum calculation are shown in Fig. 1. The two neutrino production spectra are given for an interstellar hydrogen density of  $1 \text{ cm}^{-3}$  so that it is really a production rate per hydrogen atom. The upper neutrino curve and the  $\gamma$ -ray production spectrum shown in the figure are calculated using a primary cosmic ray spectrum  $I_p(E) = 2.35 E^{-2.67} \text{ cm}^{-2} \text{ s}^{-1} \text{ sr}^{-1} \text{ GeV}^{-1}$  for  $E_p > 10$  GeV and the lower curve is obtained for a primary spectrum  $I_p(E_p) = 2.0 E^{-2.75} \text{ cm}^{-2} \text{ s}^{-1} \text{ sr}^{-1} \text{ GeV}^{-1}$  (Ryan, Dene, and Balasubrahmanyam 1972). The  $\gamma$ -ray spectrum is for all  $\gamma$ -rays

from  $\pi^0$ -decay; the  $\nu$ -spectrum is for the  $\nu_\mu$  component. Since each pion decay results in one  $\nu_\mu$ , one  $\tilde{\nu}_\mu$  and one  $\nu_e(\tilde{\nu}_e)$ , all of roughly the same energy, the total number of  $\nu$ 's produced (although of four different types) is a factor of 3 higher than that shown for  $\nu_\mu$ 's. In this regard, it should be kept in mind that the cross section ratios given in Table 1 apply.

The production rate for  $\gamma p$  interactions has been calculated using the method of Stecker and Bredekamp (1972). As an example of the range of uncertainty, two different primary spectra were used, i.e.  $I_p(E_p) = 6.4 \times 10^{-31} (E_p/10^{11})^{-2.6} \text{ cm}^{-2} \text{ s}^{-1} \text{ sr}^{-1} \text{ GeV}^{-1}$  (Linsley 1963) and  $I_p(E_p) = 2.4 \times 10^{-31} (E_p/10^{11})^{-3.24} \text{ cm}^{-2} \text{ s}^{-1} \text{ sr}^{-1} \text{ GeV}^{-1}$  (Andrews et al. 1971). The latest analysis of the ultrahigh energy air-shower data (Hillas, private communication) gives  $I_p(E_p) \approx 4 \times 10^{-31} (E_p/10^{11})^{-3} \text{ cm}^{-2} \text{ s}^{-1} \text{ sr}^{-1} \text{ GeV}$  in the energy range  $10^8 \leq E_p \leq 10^{10} \text{ GeV}$  with indications of a flattening to  $I_p(E_p) \approx 2 \times 10^{-30} (E_p/10^{11})^{-2.3}$  in the energy range  $10^{10} \leq E_p \leq 10^{11} \text{ GeV}$ . The results of the  $\gamma p$  calculation are shown in Figure 2 for the two spectra chosen. The right-hand scale of Figure 2 also shows the diffuse background flux from this process obtained by multiplying by the factor  $c/(4\pi H_0)$  where  $H_0$ , the Hubble constant, is taken to be  $50 \text{ km s}^{-1} \text{ Mpc}^{-1}$ . This flux, which is also shown in the subsequent figures, only holds if the ultrahigh energy primary spectrum is universal, an assumption which is contradicted by the lack of an observed high energy cutoff in the spectrum (Greisen 1966, Zatsepin and Kuzmin 1966, Stecker 1968, 1978a). Thus the fluxes given may be overestimated and may actually be upper limits.

Figure 3 shows the integral galactic "pp" neutrino production spectrum.

### 3. Diffuse Cosmic Neutrino Flux

Figures 4 and 5 show the differential and integral neutrino fluxes from various sources. In figure 4, the crosshatched region marked  $\gamma_p$  is obtained from the curves shown in Figure 2. The hatched region marked  $pp(G.C. |b| \leq 10^\circ)$  is for galactic  $\nu$ -production coming from the galactic central region defined by galactic longitude  $330^\circ \leq l \leq 40^\circ$  and latitudes  $|b| \leq 10^\circ$ . The dashed line is the flux computed using the isobar-fireball (I-F) model (Stecker 1971), which is probably too low. The lines bounding the hatched region are obtained using the two "pp" production spectra shown in Figure 1. All galactic "pp" curves are normalized by assuming that 1/2 of the galactic  $\gamma$ -radiation above 100 MeV observed by SAS-2 (Fichtel et al. 1978) is from  $\pi^0$ -decay and by relating the  $\gamma$ -ray and  $\nu$  production using the results given in Figure 1. Spectral measurements indicate that  $\sim 50\%$  of the galactic  $\gamma$ -rays observed above 100 MeV are most probably from cosmic-ray electron bremsstrahlung with no associated  $\nu$ -production. The curve marked PCR (UL) is an upper limit on the  $\nu$ -flux from primordial (or "cosmological") cosmic-ray interactions obtained under the assumption that the extragalactic  $\gamma$ -ray background ( $8 \times 10^{-6} \text{ cm}^{-2} \text{ s}^{-1} \text{ sr}^{-1}$  above 100 MeV with an  $E^{-3}$  power law spectrum) is from interactions of cosmic-rays at high redshifts (Stecker 1969). A detailed comparison of the calculated and observed spectra (Stecker 1974, 1978b, Montmerle 1977) indicates that the  $\gamma$ -ray background is most probably not from PCRs so that the curve shown is an upper limit. Note that this upper limit is many orders of magnitude below the cosmological neutrino upper limit given by Berezhinsky and Zatsepin (1977 and references therein).

The curves in Figure 4 marked H(ATM) and V(ATM) are the horizontal and vertical atmospheric background fluxes given by Osborne, Said and



Wolfendale (1965), which indicate the background problems involved in detecting cosmic neutrinos.

The integral fluxes in Figure 5 show galactic "pp" fluxes for the central region  $330^\circ \leq l \leq 40^\circ$  (GC) for  $|b| \leq 2^\circ$  and  $|b| \leq 10^\circ$ , the anticenter region (AC) for  $|b| \leq 2^\circ$  and the region of the galactic poles (GP). All of these spectra were normalized using the SAS-2  $\gamma$ -ray data as presented by Fichtel et al. (1978) except for the GP curve which was obtained from Fig. 3 using a mean galactic path length of hydrogen gas  $\langle nL \rangle = 3 \times 10^{20} \text{ cm}^2$ . The atmospheric flux shown in Fig. 5 is from Zatsepin and Kuzmin (1962). The insert shows the galactic latitude distribution of neutrinos calculated for energies above 1 TeV. The curve marked "other galaxies" is obtained by assuming a density of normal galaxies of  $3 \times 10^{-76} \text{ cm}^{-3}$  (Felten 1977 and private communication) and assuming that they have the same  $\gamma$ -ray luminosity as our galaxy which is assumed to radiate 1/2 of its  $\gamma$ -ray flux from  $\pi^0$ -decay. Note that since the predicted  $\gamma$ -ray spectrum from normal galaxies is considerably flatter than the observed extragalactic background, so that the limit on the  $\gamma$ -ray flux from other galaxies due to  $\pi^0$ -decay is probably  $\sim 2 \times 10^{-6} \text{ cm}^{-2} \text{ s}^{-1} \text{ sr}^{-1}$  above 100 MeV, the  $\nu$ -background from  $\pi^0$ -decay cannot be significantly higher than the curve marked "other galaxies".

#### 4. Event Rates

The  $\nu N$  cross section rises linearly with  $E_\nu$  and is  $\sim 0.7 \times 10^{-38} E_\nu \text{ cm}^2$  at accelerator energies (Barish 1978). The  $\tilde{\nu} N$  cross sections are  $\sim 1/3$ - $0.4$  of this value (see Table 1), although there is now evidence of an increase in this ratio to  $\sim 0.6$  at  $E_\nu \sim 100 \text{ GeV}$  (Barish 1978), possibly due to a new flavor b-quark with  $m_b \sim 5 \text{ GeV}$  (Barnett 1976). Above a critical energy

$$E_\nu^c = M_W^2 / 2M_p, \quad (1)$$

where  $M_W$  is the mass of the intermediate vector boson and  $M_p$  is the proton mass, the energy dependence of the cross section levels off to a logarithmic one (Bjorken and Paschos 1970). In the unified gauge theory of Weinberg and Salam,  $M_W = 37.3 \csc \theta_W$  where  $\theta_W$  is a parameter of the theory (Weinberg 1974). The best experimentally determined value at present is  $\sin^2 \theta_W \approx 0.3$  (Barish 1978) giving  $M_W \approx 70$  GeV. The resulting  $\nu N$  cross section as a function of  $E_\nu$  is shown in Fig. 6.

Using the  $\nu N$  cross section from Fig. 6 for  $M_W = 70$  GeV (solid line) and a strictly linear cross section ( $M_W = \infty$  dashed line) together with the calculated cosmic  $\nu$ -fluxes, expected event rates for  $\nu_\mu$ 's falling on a  $1 \text{ km}^3$  seawater detector were calculated and are given in Fig. 7. The dotted line marks the level corresponding to 1 event/yr. The upper "pp" curve is for the flux from the galactic central region using the production spectrum of Fig. 3 which is derived from the upper  $\nu$ -curve of Fig. 1. The curve marked  $\langle pp \rangle_{\text{GAL}}$  is for the galactic "pp" neutrinos averaged over  $4\pi$  sr. Thus, on the average, one would expect an event rate of  $\sim 1 \text{ yr}^{-1}$  from galactic  $\nu_\mu$ 's of energy  $> 10$  TeV. If ultra high energy cosmic rays are universal (not likely) and the  $\nu N$  cross section rises linearly up to  $\sim 10^9 \text{ GeV}$  ( $M_W \gg 5 \times 10^4 \text{ GeV}$ , again not likely) this rate could again be reached for  $E_\nu > 10^9 \text{ GeV}$  from  $\gamma p$  interactions. It is more likely, however, that at energies high enough to see steady diffuse fluxes of cosmic neutrinos with a  $1 \text{ km}^3$  detector above the atmospheric background, the event rates will be very low.

##### 5. Comparison With Previous Calculations

Figure 8 shows the predicted fluxes of both  $\nu_\mu$  and  $\bar{\nu}_\mu$  coming from "pp" interactions in the galactic anticenter direction as well as the flux of

$\nu_\mu + \bar{\nu}_\mu$  from the  $\gamma p$  process. The curves are shown for the present work and the results of Silberberg and Shapiro (1977) and Margolis et al. (1978). The calculations of Berezhinsky and Zatsepin (1977), when adjusted for the anticenter region, would be similar to the results of Silberberg and Shapiro (1977). The results obtained here, as shown in Fig. 8, give pp fluxes which are roughly an order of magnitude below those obtained by Shapiro and Silberberg for the energy range  $10^2 \text{ GeV} < E_\nu < 10^7 \text{ GeV}$  and which are, on the average, roughly two orders of magnitude below those given by Margolis et al. over the energy range  $10^3 \text{ GeV} < E_\nu < 10^8 \text{ GeV}$  for galactic "pp" neutrinos. The  $\gamma p$  flux calculated here is two orders of magnitude below that given by Margolis et al. for the  $10^6 - 10^8 \text{ GeV}$  energy range. (See Appendix II).

There are three probable reasons why the fluxes given here are lower than those given previously by other authors.

1) Somewhat steeper, but more accurate, primary spectra were used in the present calculation.

2) An erroneous flattening appears in the pp results of Margolis et al. (1978) in the  $10^2 - 10^4 \text{ GeV}$  energy range. (See Appendix I).

3) Perhaps most importantly, our pp neutrino fluxes were normalized to the 100 MeV  $\gamma$ -ray observations of the Galaxy, making use of the generic relation between charged and neutral pion production (see Fig. 1).

Finally, it should be noted that existing observations of the extragalactic  $\gamma$ -ray background flux and spectrum place severe limits on cosmological cosmic-ray pion production (Stecker and Silk 1969, Stecker 1971) and therefore call into question high redshift production burst models such as those discussed by Berezhinsky and Smirnov (1975) and Berezhinsky and Zatsepin (1977). In particular, the upper limits given by these authors for the cosmological

pp and py  $\nu$ -fluxes are too high. The "pp" upper limit is that given in Figs. 4 and 5 marked PCR(UL) (see Section 3). The py upper limit is not related to the X-ray background as proposed by Berezhinsky and Smirnov (1975) because the X-ray background cannot be related to photopion production as originally proposed by Strong et al. (1973) since the shape of the  $\gamma$ -ray background spectrum above 10 MeV has the form of  $\sim E^{-3}$  whereas the model of Strong et al would give a spectrum of the form  $\sim E^{-2}$ . Furthermore, the Hillas (1967) model on which these cosmological calculations are based, implies a  $\gamma$ -ray background flux above that observed unless the mean intergalactic gas density at present is  $\leq 10^{-10} \text{ cm}^{-3}$  (Stecker 1971, 1975)<sup>1</sup>, well below that implied by recent x-ray observations of galactic clusters, and unless galaxy formation occurred at an extremely efficient rate at redshifts  $z \geq 15$ , an assumption which creates problems of compatibility with radio and optical observations (Rees 1972).

The flux of  $\nu$ 's from other normal galaxies is estimated here in Fig. 5 and discussed in Section 3. Further discussion of possible extragalactic  $\nu$ -fluxes is given by Silberberg and Shapiro (1977).

<sup>1</sup>The earlier limit of  $10^{-9} \text{ cm}^{-3}$  was obtained using older data. The presently given limit of  $10^{-10} \text{ cm}^{-3}$  is obtained using the results recently given by Fichtel et al (1978).

### References

- Andrews, D., Edge, D. M., Evans, A. C., Reid, R. J. O. and Tennent, A. M.  
1971. Proc. 12th Int'l. Conf. on Cosmic Rays, 993.
- Barish, B. C. 1978. Phys. Rpts. 39C, 279.
- Barnett, R. M. 1976. Phys. Rev. Lett. 36, 1163.
- Berezinsky, V. S. and Smirnov, A. Yu. 1975. Ap. and Space Sci. 32, 461.
- Berezinsky, V. S. and Zatsepin, G. T. 1970. Sov. J. Nuc. Phys. 11, 111.
- Berezinsky, V. S. and Zatsepin, G. T. 1977. Sov. Phys. Usp. 20, 361.
- Bjorken, J. D. and Paschos, E. A. 1970. Phys. Rev. D1, 3151.
- Eichler, D. 1978. Ap. J. 222, 1109.
- Eichten, T., et al. 1973a. Phys. Lett. 46B, 274.
- Eichten, T., et al. 1973b. Phys. Lett. 46B, 281.
- Felten, J. E. 1977. Astron. J. 82, 861.
- Fichtel, C. E., Simpson, G. A. and Thompson, D. J. 1978. Ap. J. 222, 833.
- Ganguli, S. N. and Sreekantan, B. V. 1976. J. Phys. A9, 311.
- Greisen, K. 1966. Phys. Rev. Lett. 16, 748.
- Hillas, A. M. 1967. Phys. Lett. 24A, 677.
- Linsley, J. 1963. Phys. Rev. Lett. 9, 126.
- Margolis, S. H., Schramm, D. N. and Silberberg, R. 1978. Ap. J. 221, 990.
- Montmerle, T. 1977. Ap. J. 216, 620.
- Osborne, J. L., Said, S. S. and Wolfendale, A. W. 1965. Proc. Phys. Soc.  
London 86, 93.
- Rees, M. J. 1972. in External Galaxies and Quasi Stellar Objects (ed. D. E.  
Evans) Reidel, Dordrecht, 407.
- Ryan, M. J., Ormes, J. F. and Balasubrahmanyam, V. K. 1972. Phys. Rev.  
Lett. 28, 1497.

- Silberberg, R. and Shapiro, M. M. 1977. Proc. 15th Int'l. Cos. Ray Conf., Plovdiv 6, 237.
- Stecker, F. W. 1968. Phys. Rev. Lett. 21, 1016.
- Stecker, F. W. 1969. Ap. J. 157, 507.
- Stecker, F. W. 1970. Ap. and Space Sci. 6, 377.
- Stecker, F. W. 1971. Cosmic Gamma Rays, Mono Book Corp., Baltimore.
- Stecker, F. W. 1973a. Ap. and Space Sci. 20, 47.
- Stecker, F. W. 1973b. Ap. J. 185, 499.
- Stecker, F. W. 1975. in Origin of Cosmic Rays (ed. J. L. Osborne and A. W. Wolfendale) Reidel Pub. Co., Dordrecht, 267.
- Stecker, F. W. 1978a. Comments on Ap. 7, 129.
- Stecker, F. W. 1978b. Nature 273, 4
- Stecker, F. W. and Bredekamp, J. 1972. NASA Rpt. X-641-72-480.
- Stecker, F. W. and Silk, J. 1969. Nature 221, 1229.
- Wdowczyk, J., Tkaczyk, W., and Wolfendale, A. W. 1972. J. Phys. A5, 1419.
- Weinberg, S. 1976. Rev. Mod. Phys. 46, 255.
- Zatsepin, G. T. and Kuzmin, V. A. 1962. Sov. Phys. JETP 14, 1294.
- Zatsepin, G. T. and Kuzmin, V. A. 1966. Zh. Eksp. Theor Fiz. (Pisma) 4, 114.

Table 1.  $\nu N$  Cross Section Ratios

Ratio	Experimental Value	Theoretical Value
$\sigma_{\nu_e N} / \sigma_{\nu_\mu N}$	$1.26 \pm 0.23$	1
$\sigma_{\tilde{\nu}_e N} / \sigma_{\tilde{\nu}_\mu N}$	$1.32 \pm 0.32$	1
$\sigma_{\tilde{\nu}_\mu N} / \sigma_{\nu_\mu N}$	$0.40 \pm 0.12$	$\sim 1/3^*$
$\sigma_{\tilde{\nu}_e N} / \sigma_{\nu_e N}$	$0.38 \pm 0.02$	$\sim 1/3^*$

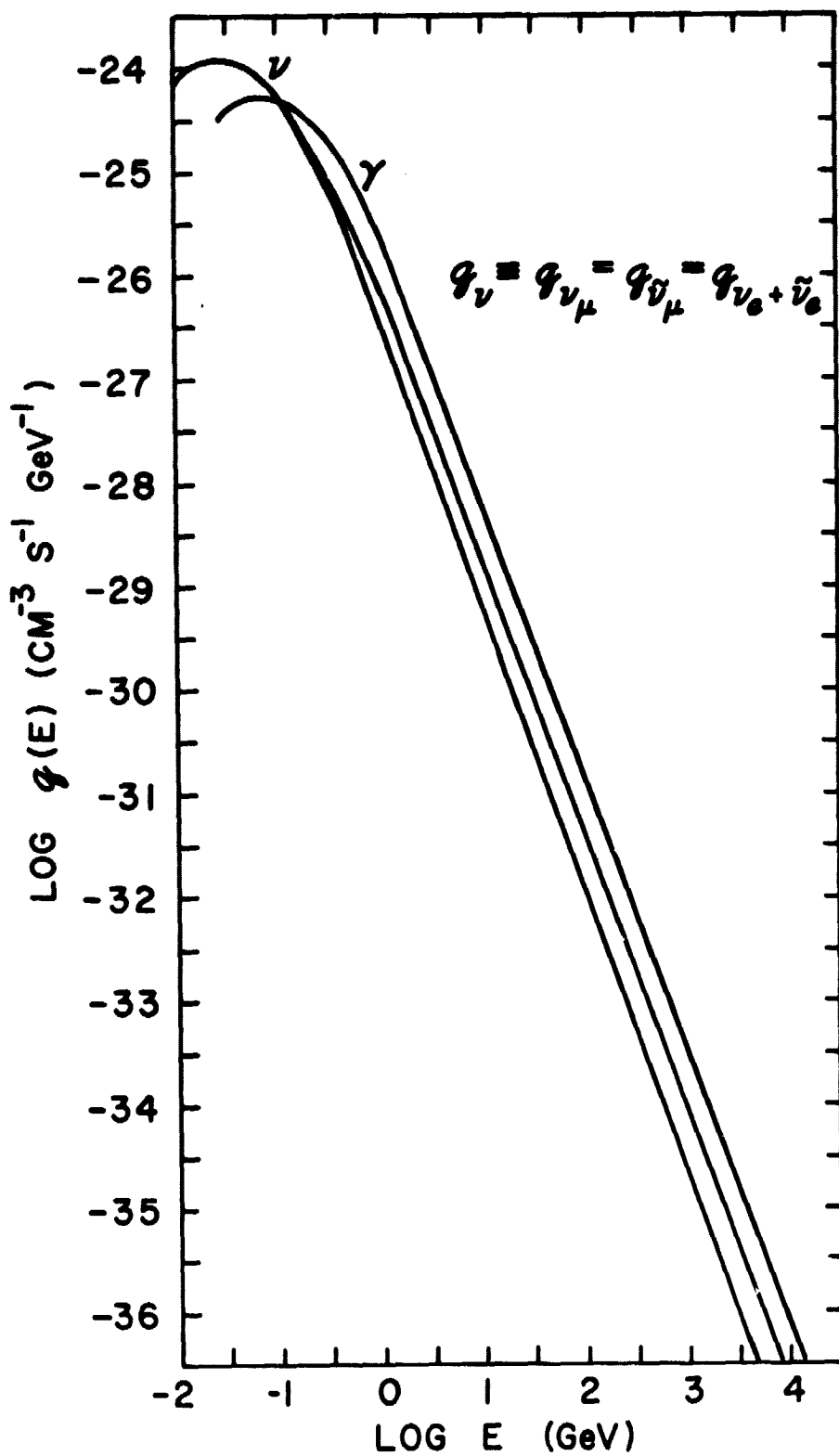
\*valence quarks dominant

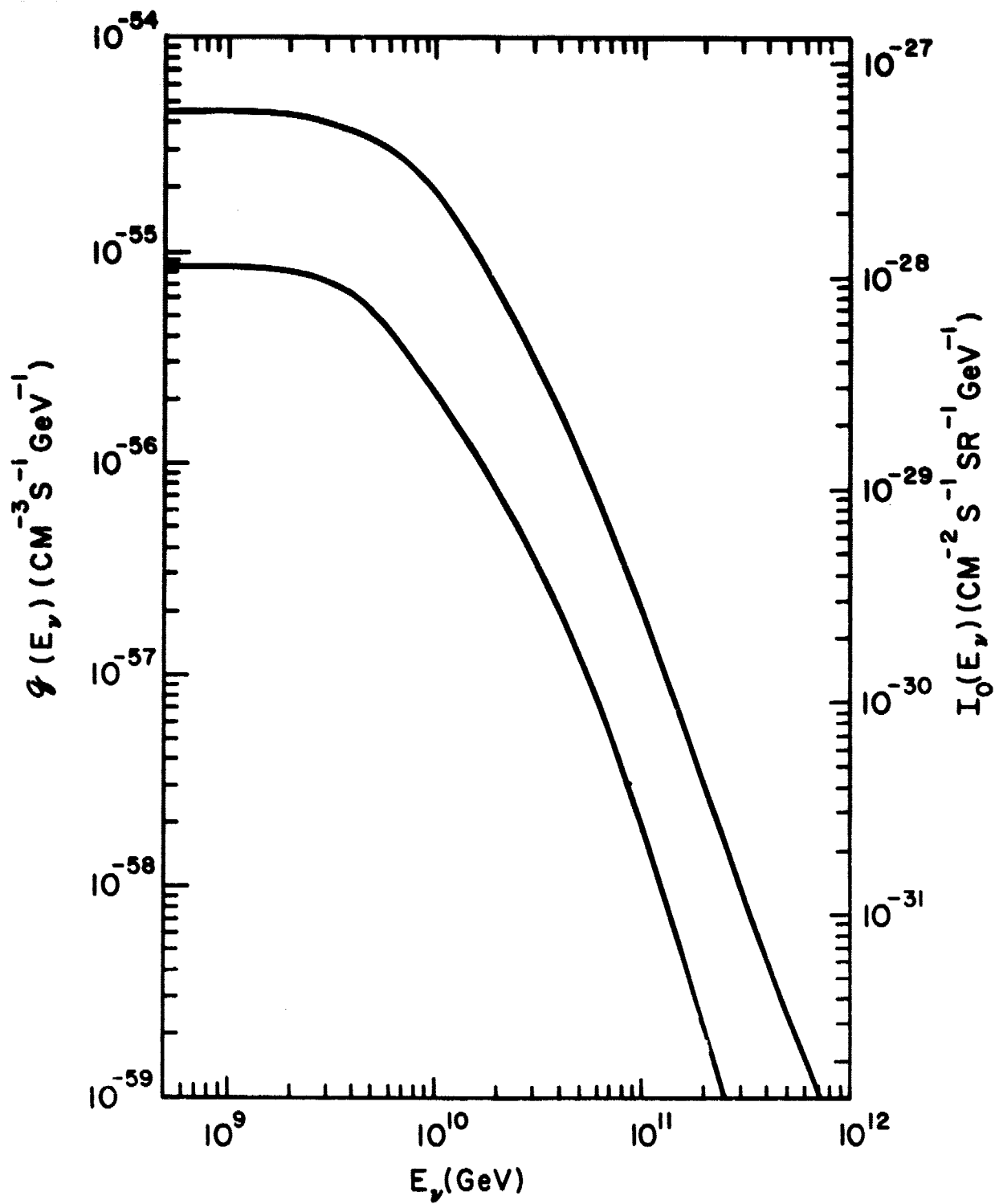
(Eichten et al. 1973a, b).

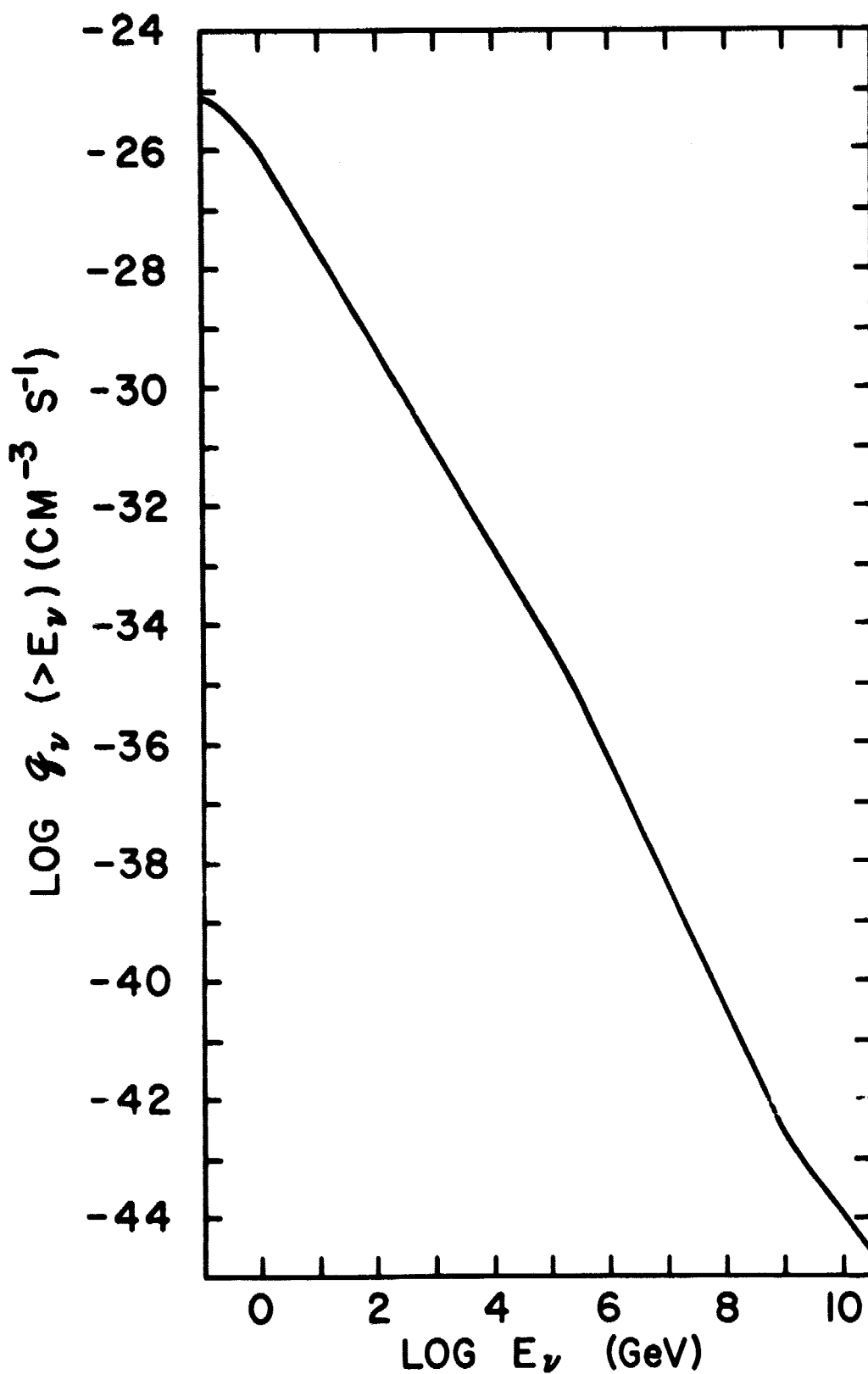
Figure Captions

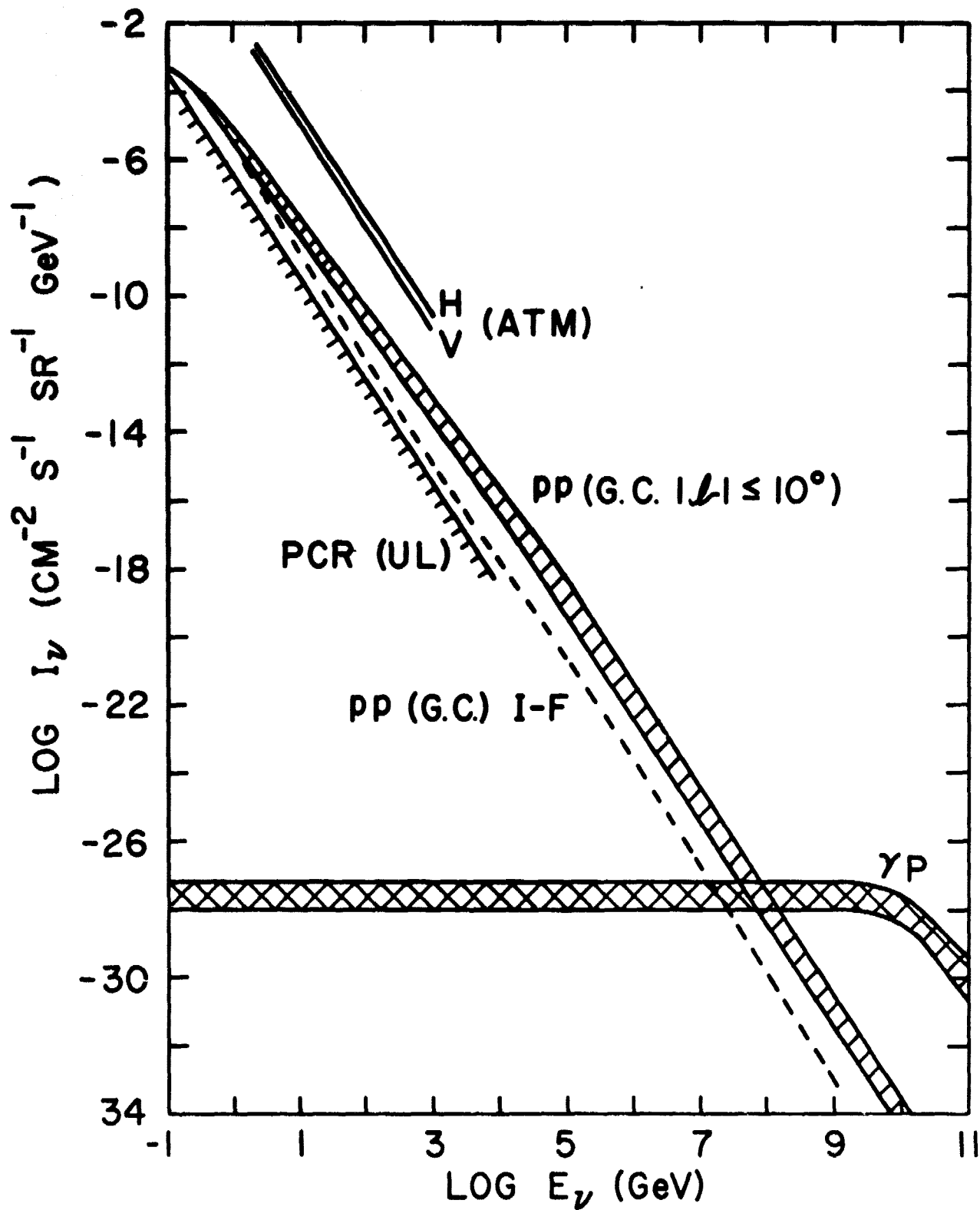
- Fig. 1. Differential production spectra of neutrinos and  $\gamma$ -rays from the decay of pions produced by interactions of cosmic-rays in our galactic neighborhood with interstellar gas having a mean hydrogen density of 1 atom per  $\text{cm}^3$ . The  $\gamma$ -ray curve and the upper neutrino curve are calculated for cosmic rays having a spectral index of 2.67 between 10 and  $3 \times 10^6$  GeV; The lower neutrino curve is for a cosmic ray spectrum with index 2.75. The spread in the curve is indicative of the uncertainty in such calculations.
- Fig. 2. Calculated differential neutrino production spectra and background fluxes from photopion production by ultrahigh energy cosmic rays interacting with the 3K universal microwave background radiation.
- Fig. 3. The integral  $\nu$ -production spectrum obtained from the upper neutrino curve in Fig. 1. The high energy cosmic ray spectrum used is from a recent analysis of Hillas (private communication).
- Fig. 4. Differential background  $\nu$ -fluxes.
- Fig. 5. Integral  $\nu$ -fluxes and the galactic latitude distribution of neutrinos with energy above 1 TeV in the direction of the inner galaxy.
- Fig. 6. Cross section for  $\nu N$  interactions assuming an intermediate vector boson mass  $M_W = 70$  GeV.
- Fig. 7. Neutrino event rates for a detector utilizing  $1 \text{ km}^3$  of water.
- Fig. 8. Comparison of present predicted neutrino fluxes with previous calculations by other workers.

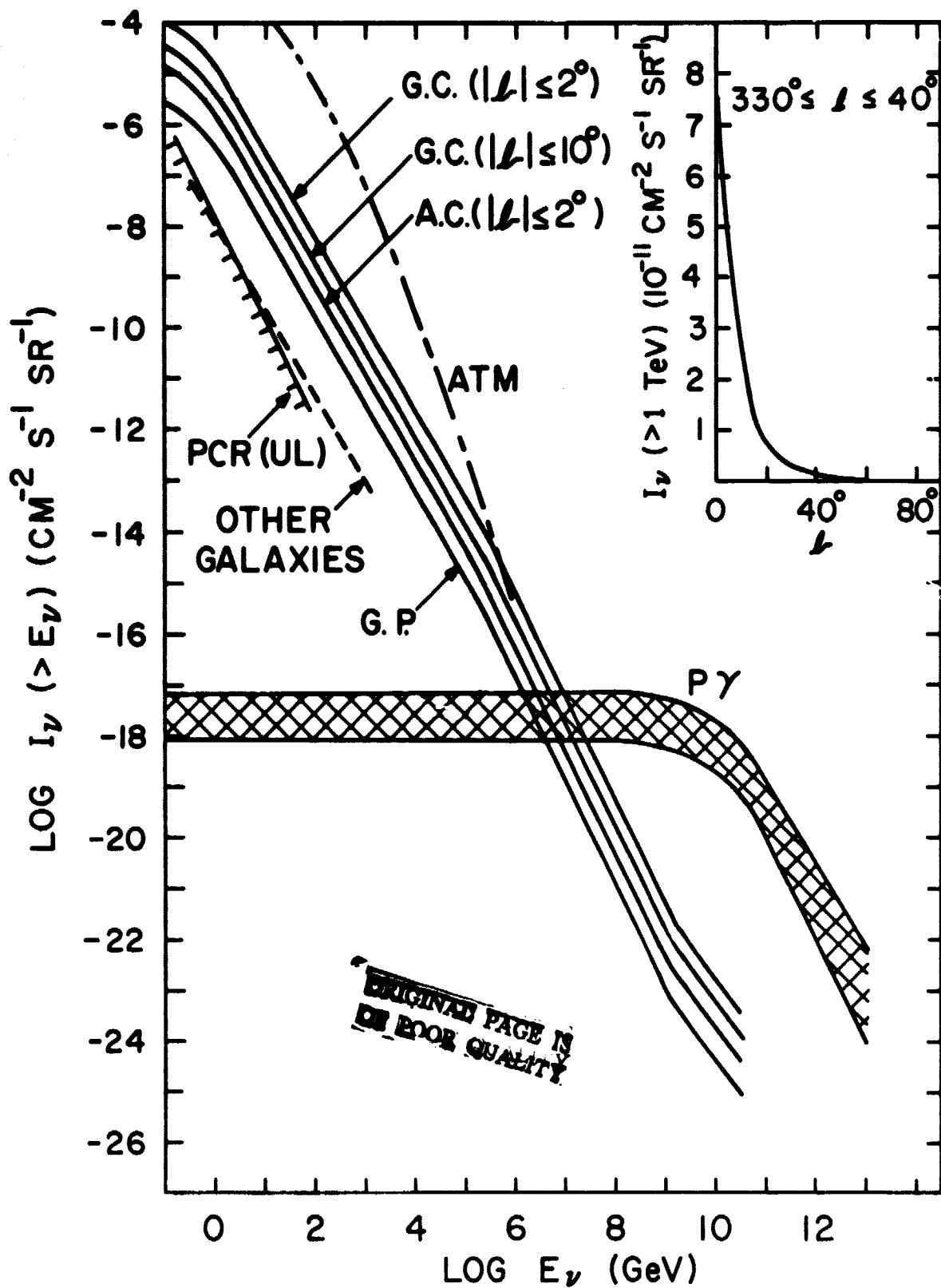


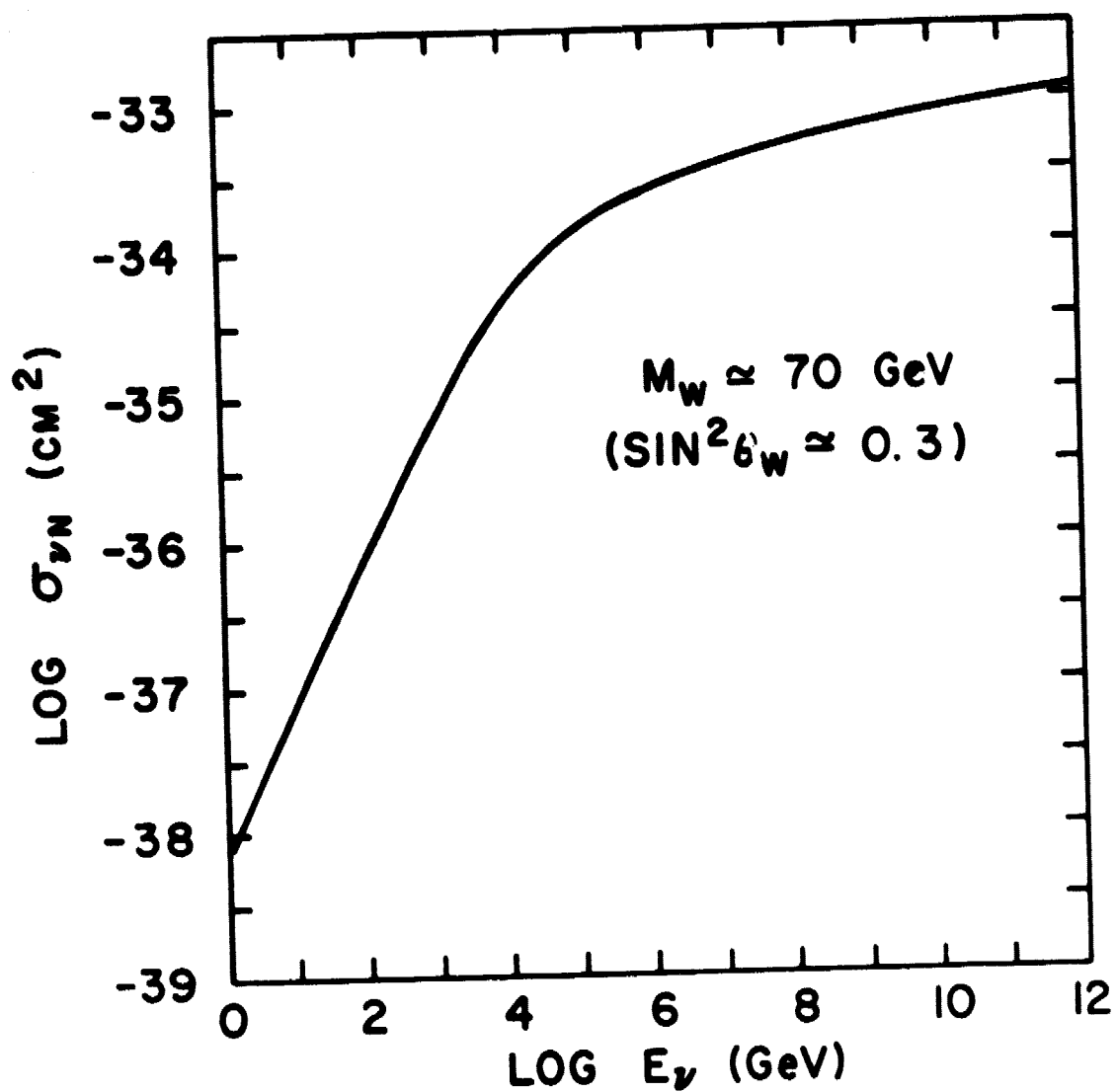


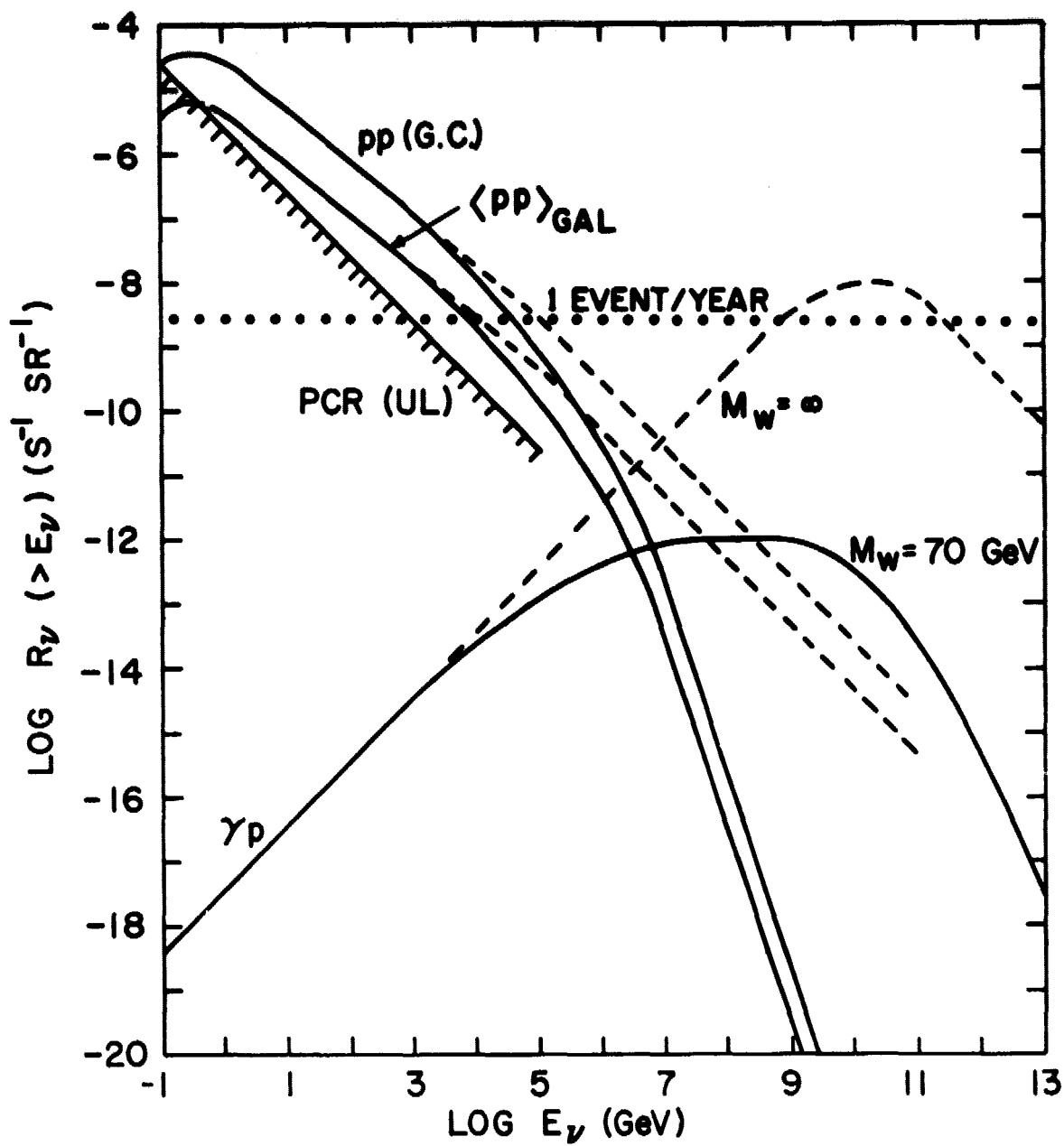


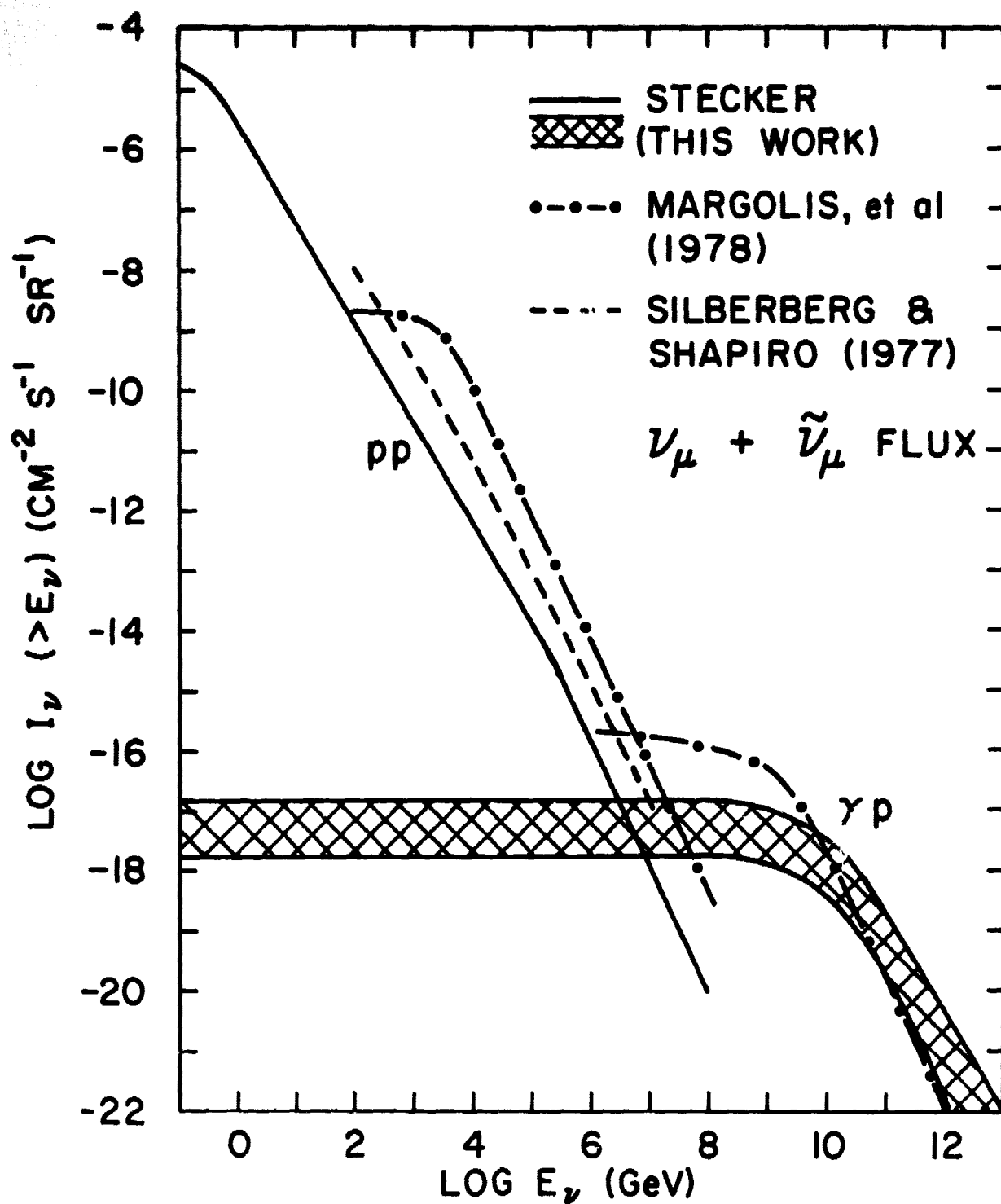














## Appendix I

High Energy Behavior of the Pion-Decay  $\gamma$ -ray and Neutrino Spectrum

Let us assume a high energy primary cosmic-ray spectrum of the power-law form

$$I_p(E_p) = K E_p^{-\Gamma} \quad (A1)$$

interacting with cosmic gas having a density  $n$  and producing secondaries observed along a line-of-sight of effective length  $L$ .

We further assume an effective production cross section for pions of average energy  $E_\pi$  produced by primaries of energy  $E_p$

$$\sigma(E_\pi | E_p) = C \zeta_0 E_p^a \delta(E_\pi - \chi_0 E_p^b) \quad (A2)$$

where  $\zeta_0$  and  $\chi_0$  are constants. Such a production function would occur for a pion multiplicity  $\zeta$  of the form  $\zeta(E_p) = \zeta_0 E_p^a$ . The secondary pion spectrum is proportional to the integral over  $dE_p$  of the product  $\sigma(E_\pi | E_p) I(E_p)$ .

In the high energy limit,  $\gamma$ -rays and neutrinos from pion decay would then have a power law form with a spectral index

$$\Gamma' = \frac{(\Gamma+b)-(a+1)}{b} \quad (A3)$$

In the case of  $\gamma$ -rays, the spectrum would be

$$I(E_\gamma) = \frac{2\langle nL \rangle K \zeta_0 C}{(\Gamma+b)-(a+1)} \chi_0^{\left(\frac{\Gamma-a-1}{b}\right)} E_\gamma^{-[(\Gamma+b)-(a+1)]/b} \quad (A4)$$

(Stecker 1971). The corresponding expression for neutrinos is somewhat more complicated.

Again, in the high energy limit, some constant fraction of the primary energy  $E_p$  goes into pions. This fraction is typically of the

order of 50%-60%, but in any case, it cannot exceed unity. It then follows that

$$b = 1-a, \quad 0 \leq a \leq 1, \quad 0 \leq b \leq 1. \quad (A5)$$

Thus, equation (A3) reduces to

$$\Gamma' = \frac{\Gamma-2a}{1-a} = \Gamma + \frac{a}{1-a} (\Gamma-2) \quad (A6)$$

In order for the total energy in cosmic rays to be finite, in the high energy limit  $\Gamma$  must be  $>2$ . In fact, observationally this is the case. Also, since  $0 \leq a \leq 1$ , it follows that

$$\frac{a}{1-a} (\Gamma-2) \geq 0, \text{ thus } \Gamma' \geq \Gamma \quad (A7)$$

i.e., the secondary spectrum has a spectral index which exceeds or equals that of the primaries.

In the case  $a = 0$ ,  $b = 1$  corresponding to the dominance of a leading pion or scaling, we find  $\Gamma' = \Gamma$  and the spectral index of the secondaries equals that of the primaries. It follows from eq. (A7) that the spectral index of the secondaries should not be smaller than that of the primaries as Margolis, et al. obtain in their scaling model calculation for the energy range  $10^2$ - $10^4$  GeV.

It is well known that if  $\pi^0$  mesons are generated with a spectrum  $g(E_\pi)$ , the  $\gamma$ -ray spectrum from their decay has the form

$$\begin{aligned} g(E_\gamma) &= \int_{E_\gamma + \frac{m_\pi^2}{4E_\gamma}}^{\infty} dE_\pi \frac{g(E_\pi)}{(E_\pi^2 - m_\pi^2)^{1/2}} \\ &\rightarrow \int_{E_\gamma}^{\infty} dE_\pi \frac{g(E_\pi)}{E_\pi} \end{aligned} \quad (A8)$$

(e.g. Stecker 1971) in the high energy limit  $E_\gamma \gg m_\pi$ . Thus if  $g(E_\pi) =$

$$K_{\pi} E_{\pi}^{-\Gamma_{\pi}}, g(E_{\nu}) = K_{\nu} E_{\nu}^{-\Gamma_{\nu}}$$

$$\text{where } K_{\nu} = K_{\pi}/\Gamma_{\pi}, \Gamma_{\nu} = \Gamma_{\pi}.$$

(A9)

It can also be easily demonstrated that the neutrinos from  $\pi \rightarrow \mu \nu$  decay also have the same spectral index as the primaries. In this case, the cms energy of the neutrino is

$$E_{\nu}^* = \frac{m_{\pi}^2 - m_{\mu}^2}{2m_{\pi}} = 29.8 \text{ MeV.} \quad (\text{A10})$$

Defining  $\eta = E_{\nu}^*/m_{\pi}$ , it follows that in the limit  $E_{\nu} \gg m_{\pi}$

$$g(E_{\nu}) = \frac{1}{2\eta} \int_{E_{\nu}/2\eta}^{\infty} dE_{\pi} \frac{g(E_{\pi})}{E_{\pi}} = \frac{1}{2\eta} \int_{2.34 E_{\nu}}^{\infty} dE_{\pi} \frac{g(E_{\pi})}{E_{\pi}}. \quad (\text{A11})$$

Again, for a power law pion spectrum of the form  $g(E_{\pi}) = K_{\pi} E_{\pi}^{-\Gamma_{\pi}}$ , the neutrino spectrum is of the form  $g(E_{\nu}) = K_{\nu} E_{\nu}^{-\Gamma_{\nu}}$  where

$$K_{\nu} = \frac{(2.34)^{-(\Gamma_{\pi}-1)}}{\Gamma_{\pi}} K_{\pi}, \Gamma_{\nu} = \Gamma_{\pi}. \quad (\text{A12})$$

The  $\pi \rightarrow \mu \nu$  decay kinematics is similar to the  $\Sigma^0 \rightarrow \Lambda \gamma$  decay kinematics discussed in Stecker (1971). The 3-body  $\mu \rightarrow e \nu \nu$  decay is more complicated but the result is also  $\Gamma_{\nu} = \Gamma_{\pi}$  (see again, Stecker 1971).

## Appendix II

Approximate  $\gamma p$  Neutrino Source Function

The main source of ultrahigh energy neutrinos is photomeson production interactions between ultrahigh energy cosmic rays and blackbody photons of the 2.7K microwave background radiation - i.e., interactions of the type  $\gamma + p \rightarrow \pi + n$ . To check on the numerical calculations presented in this paper, it is useful to derive an approximate source function for the production of neutrinos in photomeson interactions with microwave blackbody photons. We assume all the photons to be at the average energy  $\epsilon_0 \approx 2.7kT \approx 6.4 \times 10^{-4}$  eV so that

$$n_{bb}(\epsilon) = n_{bb} \delta(\epsilon - \epsilon_0), \quad n_{bb} \approx 400 \text{ cm}^{-3}. \quad (\text{B1})$$

The energy of the photon in the cosmic-ray proton rest system is

$$\epsilon' = (E_p/M_p) \epsilon_0 (1 - \cos\theta). \quad (\text{B2})$$

There is a large peak in the photomeson production cross-section at  $\epsilon' \approx 0.35 M_p$  due to the  $\Delta(1238)$  resonance and since the cosmic-ray spectrum drops off rapidly with increasing energy, most of the pion production occurs at this resonance energy. Thus, from Equation (B2) we make the approximation

$$\sigma(\epsilon') \approx \sigma_0 \delta \left[ x - \frac{0.35 M_p^2}{\epsilon_0 E_p} \right] \equiv \sigma_0 \delta(x - E_0/E_p), \quad (\text{B3})$$

where

$$x \equiv 1 - \cos\theta, \quad E_0 \equiv \frac{0.35 M_p^2}{\epsilon_0} \approx 4.8 \times 10^{11} \text{ GeV}$$

and

$$\sigma_0 \approx 2 \times 10^{-28} \text{ cm}^2.$$

Then the source function for neutrino production from  $\pi \rightarrow \mu \nu$  decay may be written in the form

$$q(E_\nu) = 4\pi/2\eta \int_{E_\nu/2\eta}^{\infty} \frac{dE_\pi}{E_\pi} n_{bb} \int_0^2 x dx \int_0^x dE_p I(E_p) \sigma(E_p, x) f(E_\pi | E_p).$$

We assume all the pions to be produced at the average energy

$$\langle E_\pi \rangle = \frac{E_p m_\pi^2 + 2\varepsilon' M_p}{2 M_p^2 + 2\varepsilon' M_p}. \quad (B5)$$

If we use Equation (B4), Equation (B5) further reduces to

$$\langle E_\pi \rangle \simeq \frac{E_p^2}{2} \frac{m_\pi^2 + 0.7 M_p^2}{1.7 M_p^2} \simeq E_p/5, \quad (B6)$$

so that the distribution function is approximated by

$$f(E_\pi | E_p) \simeq \delta(E_\pi - E_p/5). \quad (B7)$$

If we further specify the differential cosmic-ray proton spectrum by a power-law of the form  $I(E_p) = K_p E_p^{-\Gamma}$ , Equation (B4) reduces to

$$\begin{aligned} q(E_\nu) &\simeq 2\pi n_{bb} \sigma_0 K_p / \eta \int_{E_\nu/2\eta}^{\infty} dE_\pi / E_\pi \int_0^2 x dx \int_{(E_0/2)}^{\infty} dE_p E_p^{-\Gamma} \delta(x - E_0/E_p) \delta(E_\pi - E_p/5) \\ &= 10\pi \sigma_0 n_{bb} K_p E_0 / \eta \int_{\max[E_0/2, 5E_\nu/2\eta]}^{\infty} dE E^{-(\Gamma+2)} \end{aligned} \quad (B8)$$

The solution to Equation (B8) may then be written in the simple form

$$q(E_\nu) = \begin{cases} Q_\nu, & E_\nu \leq E_1 \\ Q_\nu (E_\nu/E_1)^{-(\Gamma+1)}, & E_\nu \geq E_1 \end{cases} \quad (B9)$$

where  $E_1 \simeq 5E_0/\eta \simeq 2 \times 10^{10}$  GeV and

$$Q_\nu \simeq 2.35 \times 10^{-23} K_p (E_0/2)^{-\Gamma/(\Gamma+1)} \quad (B10)$$

For example, if  $I(E_p) = 2.5 \times 10^{-2} E_p^{-2.6}$  (Linsley 1963)

$$Q_v = 4.2 \times 10^{-55} \text{ cm}^{-3} \text{ s}^{-1} \text{ GeV}^{-1}. \quad (\text{B11})$$

Equations (B9) and (B11) may be directly compared with the upper curve in figure 2 as a check on the order-of-magnitude of the calculations since our numerical results differ significantly from those of Margolis et al. (1978). The numerical results shown in Fig. 2 include the effect of meson production above the  $\Delta(1236)$  resonance. This has the effect of producing a flatter spectrum than  $E_v^{-(l+1)}$  at the highest energies, one more like  $E^{-\Gamma}$ . (Please note that eqs. (8)-(10) of Stecker (1973) contain an error in the spectral index but the effect on the results of that paper are not significant as indicated by the more accurate numerical results of Stecker and Bredekamp (1972)).